Training and Communication for Earthquake Risk Assessment

TREQ Project

Seismic hazard analysis at the urban scale

Deliverable 2.2.4 – Version 1.0.0

Global Earthquake Model (GEM) Foundation

www.globalquakemodel.org

Description of the methods used and final urban hazard results for the TREQ cities

Seismic hazard analysis at the urban scale

Deliverable D2.2.4

Technical report produced in the context of the TREQ project

Version 1.0.0 – October, 2021

R. Gee[1], C. Shreyasvi [1], M. Pagani[1]

[1]Global Earthquake Model Foundation

Collaborators

The authors would like to highlight the contribution from the Colombian Geological Survey (SGC), special thanks to Fernando Javier Díaz Parra and Monica Arcila, for their review and valuable feedback.

Additional partners participated in the discussions about the results of this work:

- Servicio Geológico Colombiano (SGC)
- Servicio Geológico Nacional (SGN) de la República Dominicana
- Instituto Geofísico de la Escuela Politécnica Nacional (IG-EPN)
- Pontificia Universidad Católica del Ecuador (PUCE)

Acknowledgements

This report forms part of the United States Agency for International Development (USAID) and the Bureau of Humanitarian Assistance (BHA) funded program for Training and Communication for Earthquake Risk Assessment (TREQ) project, grant AID-OFDA-G-720FDA19GR00273. The Global Earthquake Model Foundation manage and executes the resources of USAID and implements the project in collaboration with local stakeholders.

The TREQ Project is designed to demonstrate how earthquake hazard and risk assessment can inform decision makers in the development of risk reduction policies, as well as how earthquake risk can be properly communicated to stakeholders and the public in general. Specifically, the project aims to develop capacity for urban earthquake risk assessment in Latin America, Quito (Ecuador), Cali (Colombia), and Santiago de los Caballeros (Dominican Republic), while the second part will produce training, educational and communication materials that will enhance the understanding of earthquake risk worldwide. This program targets a wide spectrum of stakeholders, categorized into four main groups: governance (decision-makers/public authorities), industry (practitioners and professionals), academia (researchers and professors), and the community.

This report has been made possible thanks to the support and generosity of the American people through the United States Agency for International Development (USAID) and the Bureau of Humanitarian Assistance (BHA). The opinions, findings, and conclusions stated herein are those of the authors and do not necessarily reflect the views of USAID or the United States Government.

Citation: R. Gee, S. Chandrasekhar, M. Pagani (2021). Seismic hazard analysis at the urban scale. GEM-TREQ project technical report, deliverable D.2.2.4, v1.0.0, October 2021.

http://www.globalquakemodel.org/

CONTENTS

1 EXECUTIVE SUMMARY

We perform seismic hazard analysis for three urban centers (Cali, Colombia; Quito, Ecuador; and Santiago, Dominican Republic) within the TREQ project, explicitly accounting for the local soil response in each city. The two requirements for this analysis are (1) hazard estimates on reference bedrock at each city, for which we use the models described in D2.2.2 and D2.2.3 and (2) soil response models that quantify the amplification (or deamplification) of ground shaking throughout the three urban centers due to the shallow soil layers. In this study, in collaboration with local experts, we develop the soil response models for each city using available local geotechnical and geophysical data. We simulate the soil response using 1D equivalent linear analysis using pySRA, and a large suite of input motions generated from (and therefore fully compatible with) the underlying hazard model, which accounts for uncertainty in the input motions. The computed soil response models consist of a set of soil amplification factors (AF) and their uncertainty ($\sigma_{\ln AF}$), covering the respective urban centers. The AFs are defined for periods relevant for risk analysis (PGA – 2.0 s), as well as for a wide range of bedrock shaking intensity levels (0.05 – ~4 g), and can therefore be readily used for probabilistic hazard and risk analysis. Finally, hazard curves are computed at the surface by convolving the bedrock hazard with the AFs and $\sigma_{\ln AF}$ at a set of sites. The results are compared to those computed using the ergodic site terms within the GMPEs, which depend on the shear wave velocity in the upper 30 m (Vs30), for which we find significant differences at some sites. Specifically, using the local soil response models can either increase (up to a factor ~2) or decrease the hazard results compared to when an inferred Vs30 is used. For soft sites at longer return periods, the hazard can be lower (and sometimes lower than the hazard on rock) due to soil nonlinearity. These differences can have a significant impact on the risk results, which are described in Deliverable D2.3.5. This study demonstrates the importance of incorporating local soil response when the goal is to model hazard at the urban scale with a higher level of detail compared to more standard approaches using Vs30.

2 INTRODUCTION

Latin America is one of the most seismically active parts of the world and also one of the most urbanized, with 81% of the population living in cities (UN, 2019). The concentration of people, buildings, and economic value in seismic regions leads to an increased risk, but it also poses unique challenges from a hazard modelling perspective. Urban centers are often built on sedimentary basins, which provide flat terrain for building, but are well known to alter seismic waves resulting in potentially more damaging ground motions compared to those observed on rock. These "site-effects" are usually approximated, or not considered at all, when performing national or regional scale seismic hazard analysis. Working at the urban scale allows for more comprehensively taking into account these effects.

There are two main approaches for modelling site response in seismic hazard analysis. The first, and most common, is to model site response through generic ergodic amplification functions within GMPEs (e.g., Kamai et al., 2014), which commonly use the Vs30 parameter as a proxy for site response. This is generally used for national or regional scale analyses since Vs30 can readily be estimated from surface topography (Allen and Wald, 2007; Heath et al., 2020). While practical, this approach cannot always capture all aspects of the site response, such as resonance effects and soil nonlinearity. The second approach requires local geotechnical or geophysical data and involves explicitly modelling the soil response, and then either adjusting the hazard model or the hazard results on reference bedrock, for which various methods have been proposed (for a review, see Aristizábal et al., 2016). This is commonly used for site-specific studies, where a higher level of detail is required when modelling the soil response. Microzonation (MZ) studies also follow the second approach to soil response modelling, however these studies do not typically compute probabilistic hazard results, but are instead more focused on identifying zones with homogeneous seismic behavior and providing seismic design actions (e.g., SM Working Group, 2015).

For the TREQ project, we follow the second approach and develop local soil response models and use them to compute seismic hazard for the three cities (Cali, Quito and Santiago), in collaboration with local partners. The TREQ cities are all highly populated (> 1 million residents) and located in regions of medium-high seismic hazard, characterized by having peak ground accelerations (PGA) with 10% probability of exceedance (POE) in 50 years > 0.35 g (Pagani et al., 2020). The goal of this work is to more accurately estimate hazard (and therefore risk) compared to standard approaches that rely on Vs30, and to develop and demonstrate a methodological workflow that could also be applied to other cities. The results of this task (i.e., soil response models and hazard estimates) are the foundation for other applications within the TREQ project, such as risk analysis, and scenario and liquefaction analysis for the three cities.

3 Overview of the Cities

3.1 Cali

Cali, with a population of ~2.2 million, is the third largest city in Colombia, and has the highest seismic hazard of the major metropolitan centers in Colombia. Earthquakes from the subduction intraslab have caused the majority of damage to the city in recent history, although the city is also affected by subduction interface and shallow crustal earthquakes. Cali is located in a basin between the Cordillera Occidental to the west and the Rio Cauca to the east. The basin deposits are mainly composed of clay and silty soils and materials of volcanic origin, and the thickness of the deposits increase from west to east, reaching hundreds of meters in the east of the city (Ingeominas and Dagma, 2005).

In this study, seismic hazard on reference bedrock is computed using the official national model by Arcila et al. (2020), augmented to include the nearby Cauca-Cali-Patia fault. The details of this model can be found in Deliverable D2.2.3. The hazard in Cali on reference bedrock (Vs30=800 m/s) is shown in Figure 1. The PGA with a 10% POE in 50 years on rock is nearly constant throughout the city, ranging from 0.35 g in the southeast to 0.4 g in the northwest, the lowest of the three TREQ cities.

Previous MZ and MZ-related studies in Cali include Ingeominas and Dagma (2005), which performed an extensive MZ for the entire city, Castro Villamarín (2011), which focused on the non-linear soil response in the Cañaveralejo region, and CI Ambiental (2019) which expanded the 2005 study to include risk analysis. In this project we use the geotechnical data and zonation from Ingeominas and Dagma (2005) provided by the Colombian Geological Survey. We collect geotechnical data at 39 stations and the city is divided into 10 microzones, which encompass 98% of the exposure considered in this study (Figure 1). The majority of the exposed occupants, buildings, and economic value is located in zone 6.

3.2 Quito

Quito, with a population of ~2.0 million, is the capital of Ecuador and is located in a narrow valley in the Andes bounded by active faults. The majority of historically damaging events have come from the inter-Andean valley (i.e., shallow crustal earthquakes), although subduction-related earthquakes, such as the recent 2016 Mw 7.8 Pedernales earthquake, have also been felt in Quito. The city is located in the Quito basin which mostly consists of material of volcanic origin of Middle Pleistocene age from the nearby Pichincha and Atacazo volcanic complexes, and also fluvial and alluvial deposits (Villagómez, 2003).

In this study, seismic hazard on reference bedrock is computed using the national model of Beauval et al. (2018). We use a single source model branch, which was selected because it incorporates fault sources in the proximity of Quito (i.e., the "Fault Model", see Beauval et al., 2018; Figure 11). The details of this model can be found in Deliverable D2.2.3. The hazard in Quito on reference bedrock (Vs30=800 m/s) is shown in Figure 1. The PGA with a 10% POE in 50 years on rock ranges from 0.5–0.55 g throughout the city.

Numerous MZ and MZ-related studies have been performed in Quito going back to the 1990s (e.g., EPN et al., 1994; Guéguen, 1997; ERN, 2012; Leon, 2018). In this project we use the geotechnical data and zonation from ERN (2012). We collect geotechnical data at 13 stations and the city is divided into 13 microzones, which encompass 92% of the exposure considered in this study (Figure 1). The majority of the exposed occupants, buildings, and economic value is located in zones MSQ2, MSQ10, and MSQ11.

3.3 Santiago

Santiago, with a population of ~1.2 million is the second largest city in the Dominican Republic, situated between the obliquely converging Caribbean and North American plates. Shallow crustal earthquakes pose a significant threat to the city, notably those that could occur on the Septentrional Fault which is located only 5 km north of the city, in addition to subduction earthquakes. Santiago is located within

the Cibao Valley, which is characterized by a flat relief and simple stratigraphy with neogenic and quaternary materials that are mostly clay (Llorente et al., 2017).

In this study, seismic hazard on reference bedrock is computed using the national model developed within the TREQ project (see Deliverable D2.2.2) The hazard in Santiago on reference bedrock (Vs30=800 m/s) is shown in Figure 1. The PGA with a 10% POE in 50 years on rock ranges from 0.4 g in the southwest part of the city to 0.7 g in the northeast part of the city, due to the proximity to the Septentrional Fault. The variation of hazard across the city, and also the maximum value of hazard, is greater in Santiago compared to the other cities.

To our knowledge, very few MZ and MZ-related studies have been performed in Santiago. One notable study is Roullé et al. (2011), and in this project we use the geotechnical characterization and zonation from that study. Roullé et al. (2011) used data from 54 SPT drillings and 203 geophysical measurements (from spectral analysis of surface waves and microtremor) and divided the city into 10 microzones, which encompass 99% of the exposure considered in this study (Figure 1). For each zone (with the exception of zone 8), Roullé et al. (2011) defined a representative soil column and assigned geotechnical properties to each layer, which we use in this study. The majority of the exposed occupants and buildings are in zones 0, 1, and 6, and the majority of economic value is located in zone 8.

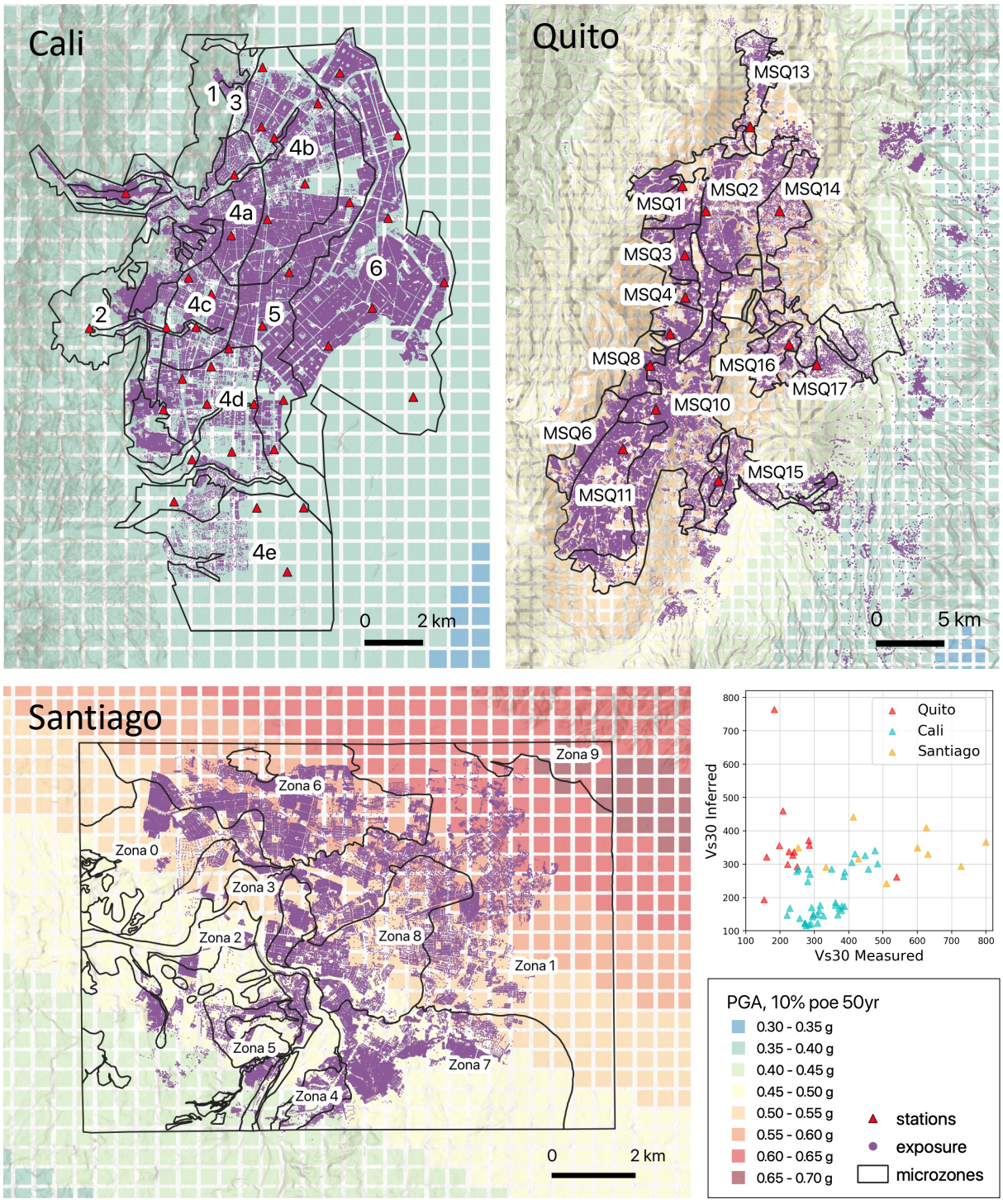

Figure 1: Hazard maps on rock (Vs30=800m/s) for Cali, Quito, and Santiago showing PGA with 10% POE in 50 years, along with microzones, stations and exposure considered in this study. In Quito there are additional assets outside the limits of the figure to the northwest. For each city, the measured versus inferred Vs30 (from Heath et al., 2020) is also plotted in the inset.

4 GEOTECHNICAL DATA

Geotechnical information was collected from the most recent and publicly available MZ studies with the help of local governmental agencies. First, the parameters needed for site response analysis (see Section 5.1), were digitized and compiled in a standard format for every layer in every soil column. This includes the layer thickness, shear wave velocity (Vs), unit weight (γ), plasticity index (PI), soil classification following the Unified Soil Classification System (USCS) and water table depth. Next, the data was homogenized to account for any missing values and differences in measured units. Finally, the profiles were extended down to the reference bedrock condition for which the hazard is computed, which is defined as the depth when Vs=800m/s is reached (see "Input motion on reference bedrock"). Two methods are used to extend the profiles. The first relies on computing the stress-normalized Vs (used in Cali), and the second follows the EPRI (2013) recommendations (used in Quito). The data and collection process for each city is described in more details below.

4.1 Cali

The geotechnical data necessary for performing urban hazard analysis comes from the 2005 MZ study (Ingeominas and Dagma, 2005), and was provided in digital format by the Colombian Geological Survey. The MZ study divided the city of Cali into 10 microzones (Figure 1) based on the geological and local site amplification characteristics. The original MZ includes 41 sites. In the present study, only 39 sites are considered since the data in zone 3 is only appropriate for 2D modelling, which is out of the scope of this analysis. Since the microzones consist of more than one site, there is more information about the spatial variation in the local soil response in Cali compared to Quito and Santiago. The measured Vs30 at the sites ranges from 220–484 m/s (Figure 1), and the digitized profiles extend down to 40–130 m (Figure 3).

Any layers with missing parameters are estimated subsequently in the homogenization step. In the shallow layers, we use the USCS (when available) to estimate the missing values of PI and γ. If the USCS is not available, which is mostly the case in the deeper layers although sometimes also in the shallow layers, we use the empirical correlations developed by Mayne (2001) (eq. 32) and Moon and Ku (2016) (eq.10). These studies have attempted to correlate the various geotechnical parameters Vs to γ and PI. Profiles missing Vs values were excluded from the analysis.

All of the profiles in Cali need to be extended to reference bedrock, for which we use the stress–normalized Vs method (e.g., Moon and Ku, 2016), which was also used in the MZ study (Ingeominas and Dagma, 2005). In this method, the Vs profiles are extended using equation 1. The vertical stress at each layer and the atmospheric pressure (101.3 kPa) are the two additional parameters required. The constant K is a soil parameter and is calculated from the overlying layers.

The resulting profiles are characterized by a decreasing Vs gradient with depth (i.e., the curves steepen with depth); therefore, when using this method it is necessary to manually impose the bedrock at specific depths otherwise the profiles extend to unrealistic depths before reaching the reference Vs horizon. Hence, the method is suitable only when the depth to bedrock is known. In Cali, estimates of

the Quaternary (Vs > ~450 m/s) and Tertiary (Vs > ~1000 m/s) deposits are provided for each site (Ingeominas y Dagma, 2005, Informe 5.2, Table 4.26), and we use the boundary between the two as the reference bedrock depth. The extended profiles using this method are presented in Figure 3, and some profiles extend to a depth of 1750 m, the deepest of the three cities. The other soil parameters are extrapolated to the reference bedrock using the methods from the homogenization stage.

4.2 Quito

The MZ study was conducted for the city for Quito and the results are presented in ERN (2012). The study divides the entire city into 13 microzones based on the geological and geotechnical characteristics as shown in Figure 1. The original MZ includes 34 sites located within the 13 microzones. In the present study, only 13 sites are considered because not all geotechnical parameters are available at the other sites (notably the sites from the "metro" study are excluded, in addition to station MSQ12 where Vs is not available). Hence each zone is represented by a single site.

The bore logs were digitized using WebPlotDigitizer-4.2 (https://automeris.io/WebPlotDigitizer). The digitization was performed at 2.0 m depth intervals rather than digitizing broad, simplified layers which do not correspond to the depths of the measurements, and are not always easily identifiable. A sample bore log is shown in Figure 2. Moreover, soil columns that are defined too coarsely have been shown to underpredict the site response as short frequencies (Kaklamanos et al., 2020). The measured Vs30 at the sites ranges from 153–540 m/s (Figure 1), and the digitized profiles extend down to 20-30 m (Figure 3).

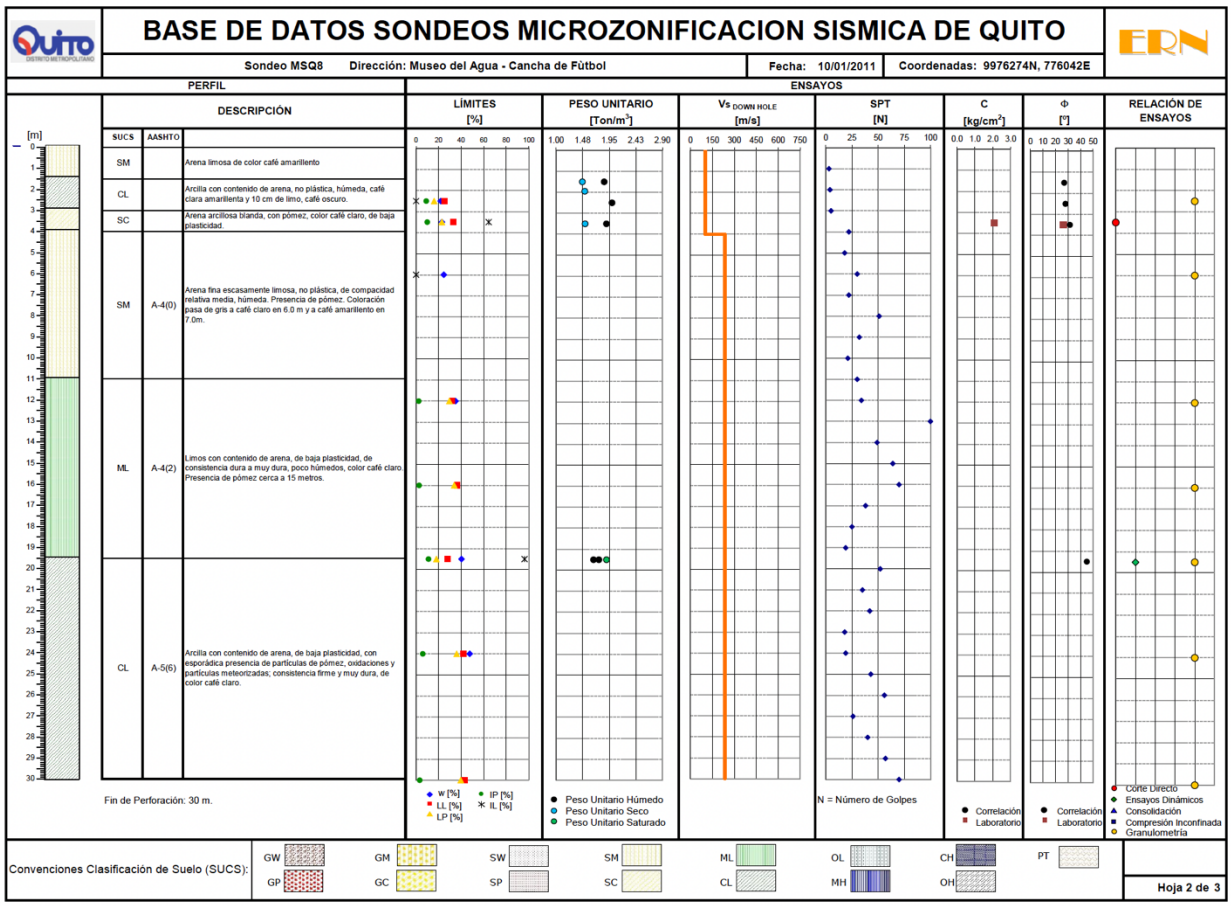

Figure 2: Example of a bore log in Quito at site MSQ8 from ERN (2012).

At all sites, the profiles do not reach reference bedrock and therefore need to be extended down. In Quito we opt to follow the EPRI (2013) guidelines, and use their recommended template profiles for extrapolating the profiles. We use this method because there is no clear indication of bedrock at most sites in Quito, and the template profiles provide a rough estimate of bedrock depth. First a template profile from EPRI (2013) is determined for each site based on the Vs at the surface. Then, the Vs gradients associated with the templates are used to extend the down the respective profiles. Since the bedrock depth is unavailable, the Vs profiles are extended until reaching Vs = 800ms-1. The extended Vs profiles for Quito are shown in Figure 3, and the deepest profiles extend to a depth of 950 m. The other soil parameters are extrapolated to the reference bedrock using the methods from the homogenization stage (as described in Section 4.1).

4.3 Santiago

The geotechnical data for Santiago was digitized from the 2011 MZ study (Roullé et al., 2011). The MZ study divided the city of Santiago into 10 microzones (Figure 1) based on the geological and geophysical characteristics. For each zone, Roullé et al. (2011) defined a representative soil column and assigned

geotechnical properties to each layer, which we use in this study. The report contains the soil columns in a tabulated form, including all necessary parameters, and the profiles extend down to bedrock. Hence, there is no need for homogenization and extension of the soil profiles. The deepest profiles extend down to 100 m (Figure 3), and the measured Vs30 at the sites ranges from 253–800 m/s.

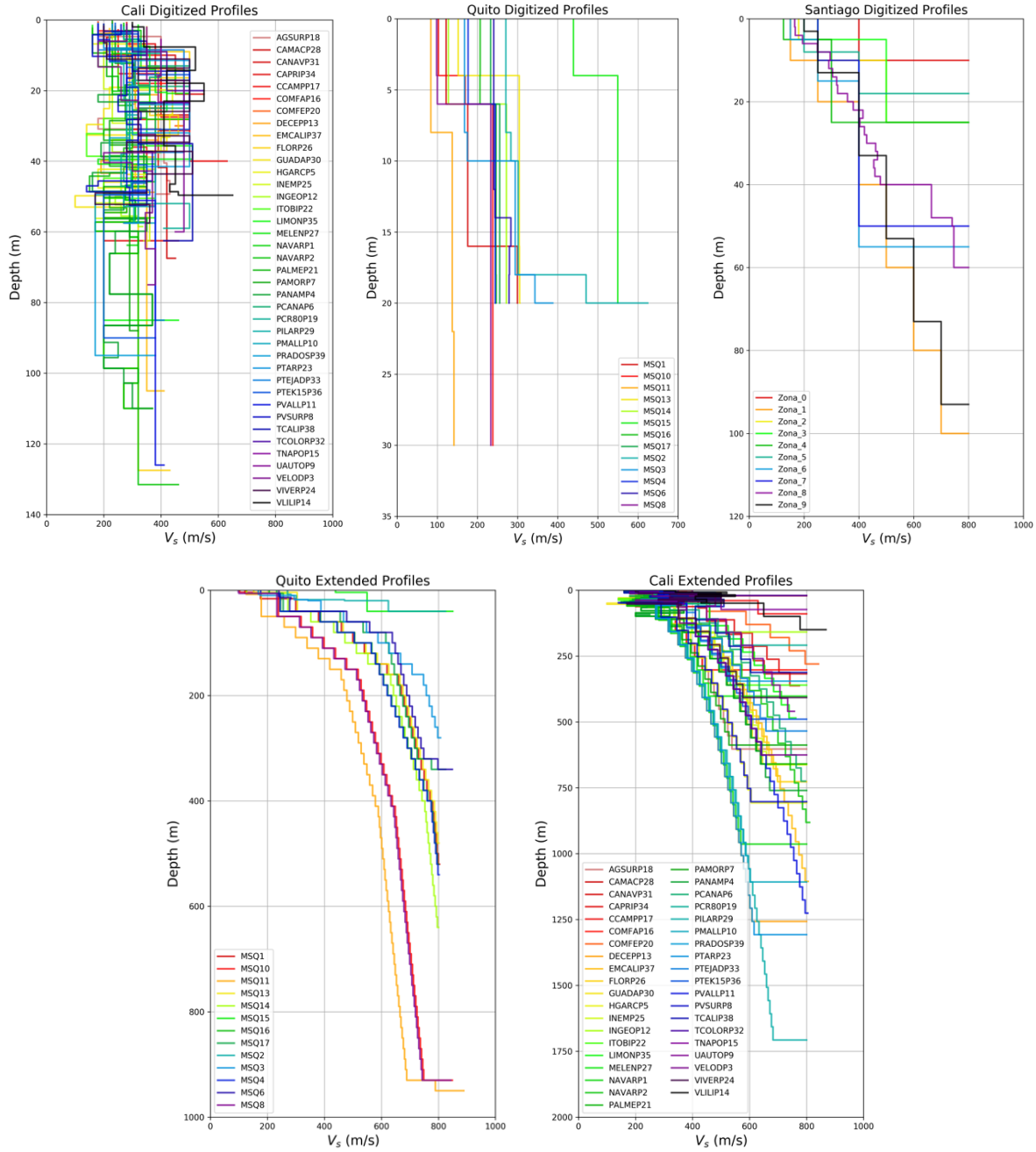

Figure 3: Top row: Digitized Vs profiles in Cali (39 profiles, data from Ingeominas and Dagma, 2005), Quito (13 profiles, data from ERN, 2012), and Santiago (10 profiles, data from Roullé et al., 2011). Bottom row: Vs profiles extended to reference bedrock (Vs = 800 m/s) in Cali and Santiago.

5 METHODOLOGY

5.1 Developing the soil response models

5.1.1 Overview of the method

We developed and applied the same methodological workflow to all three cities to generate the soil response model (Figure 4). The two inputs to the workflow are the seismic hazard model and (described in Section 3) geotechnical data (described in Section 4). The seismic hazard model is used to generate the bedrock input motions needed for SRA, which is possible because we use the random-vibration theory (RVT) approach (Rathje and Ozbey, 2006; Kottke and Rathje, 2013) which is commonly used for sites-specific hazard analyses (e.g., Rodriguez-Marek et al., 2014, 2017; Ameri et al., 2017; Tromans et al., 2019). The main benefit of this approach (in addition to eliminating the need for selecting and scaling time-series) is that we are able to consider many scenario events, and therefore cover a wide range of ground shaking intensities in our soil response model, which is important to accurately estimate hazard and risk at many return periods.

The final output for each city is a soil response model in the format compatible with the OpenQuake (OQ) Engine (Pagani et al., 2014). This is essentially a .csv file containing soil amplification factors (AF) and their uncertainty (σ_{lnAF}) for different spectral periods and input ground shaking intensity levels. Each AF is defined as the spectral ratio of the surface motion to the rock input motion ($Sa_{surface}/Sa_{rock}$), and σ_{lnAF} is the standard deviation of the logarithm of the AFs. An example of the soil response model in OQ format can be seen here.

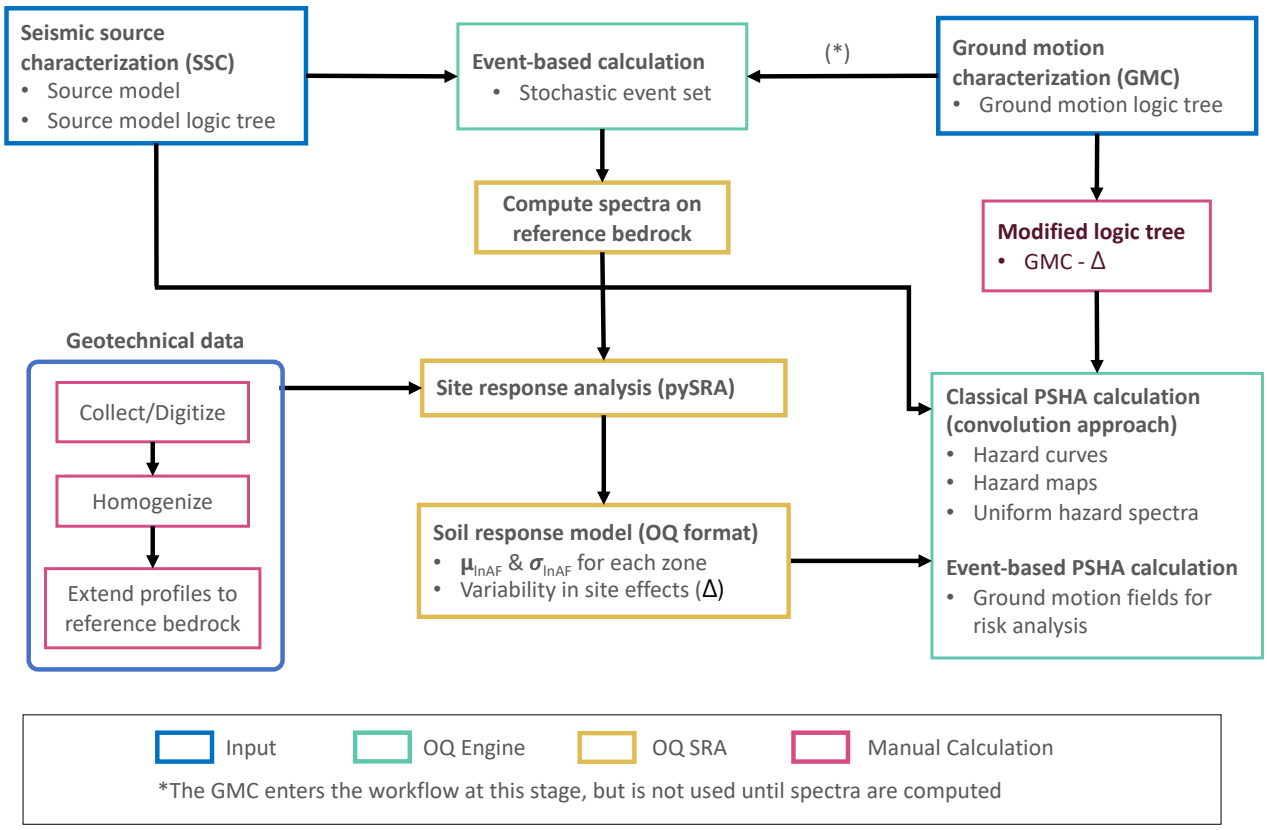

Figure 4: Schematic diagram showing the methodology used in this study, which first involves developing the soil response model, then using it in the OQ Engine to compute urban hazard (and risk) for the three cities

5.1.2 Input motions on reference bedrock

A fundamental requirement of any SRA are the input motions at the reference bedrock below the site (or in our case, the city). The RVT-based approach requires that each input motion be defined in terms of its Fourier amplitude spectrum (FAS) and a ground motion duration. Since a FAS can be derived from an acceleration response spectrum via inverse RVT (e.g., Rathje et al., 2005), we use acceleration response spectrum for the input motions, which can be easily generated from the underlying hazard model.

For each city, the first step is to generate a stochastic earthquake catalog from the seismic source model, and associate rupture properties with every event such as magnitude, hypocentral location, and tectonic region. In this analysis we use a 100,000-year catalog to ensure that a sufficient number of large, infrequent events are included. We limit the spatial extent of the catalog to 300 km around the center of each city. For each event, a GMPE is selected from the ground motion logic tree (for the same tectonic region) using a weighted random sampling based on the logic tree weights. Using the GMPE and rupture properties, the acceleration response spectrum is computed. A random sampling is performed to ensure that ground motion variability is taken into account considering values ± 3 standard deviations above and below the median ground motion.

The acceleration response spectra are computed on reference bedrock, which is defined in this study as the depth at which Vs30 reaches 800 m/s. The reference bedrock represents the top of the elastic half space in the SRA where we compute the reference motion. We use 800 m/s because it is the value for which all GMPEs used in the TREQ project are able to extend up to. This was a pragmatic choice, and a more precise value should be used in future work if more detailed information is available about the bedrock, along with host-to-target adjustments to ensure the GMPE predictions are more consistent with the expected motion on bedrock below the city.

Each acceleration response spectrum represents one possible input motion at the reference bedrock to be used for SRA. A final filtering is performed to keep the number of SRA simulations to a reasonable number. We find that using 20 randomly selected response spectra within every 0.05 g interval is sufficient to obtain stable AF estimates across all intensities. After filtering, between 700–900 input motions are used for SRA depending on the city.

5.1.3 Site response analysis

We perform SRA using pySRA (https://github.com/arkottke/pysra), which is the Python implementation of Strata. pySRA implements the 1D equivalent-linear approach, where the soil response is treated as linear, but the dynamic properties of the soil (i.e., shear modulus and damping) are updated based on the strain level at each layer in order to capture the non-linear soil behavior. More details about the software can be found in the Strata manual (Kottke and Rathje, 2009).

For each city, the suite of input motions is propagated through every soil column to obtain the surface motions. The non-linear behavior of soils is modelled using the modulus reduction and material damping curves of Darendeli (2001), which are applicable for a wide range of soil types, and take into account the influence of PI, overconsolidation ratio (OCR), which we assume to be 1, and mean effective stress, which is taken as 2/3 the effective vertical stress at each layer and accounts for the water table depth at each site. Additionally, we use the Menq (2003) model for sand and gravel layers in Cali. We use the frequency-dependent moduli and damping method (Kausel and Assimaki, 2002), to avoid obtaining unrealistically low ground motions at high intensities. The AFs are then computed by dividing the computed surface motions by the respective input motions, for each period of interest. An example of simulated AFs using the same input motions at two different sites (one stiff and one soft) is shown in Figure 5. AFs > 1 indicate amplification, and AFs < 1 indicate deamplification.

5.1.4 Calculation of AFs and σ_{lnAF}

In order to use the SRA results in the hazard calculations in the OQ Engine, we must define the median AF and $\sigma_{\ln AF}$ as a function of bedrock shaking intensity for each spectral period considered. The median AF is computed using a locally weighted scatterplot smoothing (LOWESS) regression, which is a non-parametric regression suitable for fitting a smooth curve to data points. We use this type of regression because we find that it better captures complex responses, such as soil hardening and softening (e.g., Figure 5b at 1.0 s), compared to parametric equations (e.g., Stewart et al., 2014). The following LOWESS

parameters are used: fraction (of the data used when estimating each y-value) = 0.1 for periods < 1.0 s and fraction = 0.3 s for all other periods, and the number of residual-based reweightings to perform = 0 for all periods. Using the best-fit AFs, we compute the AF residuals and the standard deviation of the logarithm of the residuals AFs (σ_{lnAF}) as a function of bedrock intensity.

The AFs are then extrapolated to large intensities (in this study ~4 g) needed for hazard and risk calculations. This is especially important for constraining hazard curves at low probabilities of exceedance (i.e., high levels of ground shaking). We use linear extrapolation if the AFs trend downward at large intensities (the majority of cases), and nearest neighbor if the AFs trend upward at large intensities (e.g., Figure 5a, at 0.6 and 1.0 s). The latter is used to prevent the extrapolated AFs from being unrealistically large. A similar procedure has been used in other studies to place an upper bound on the AFs (e.g., Rodriguez-Marek et al., 2017).

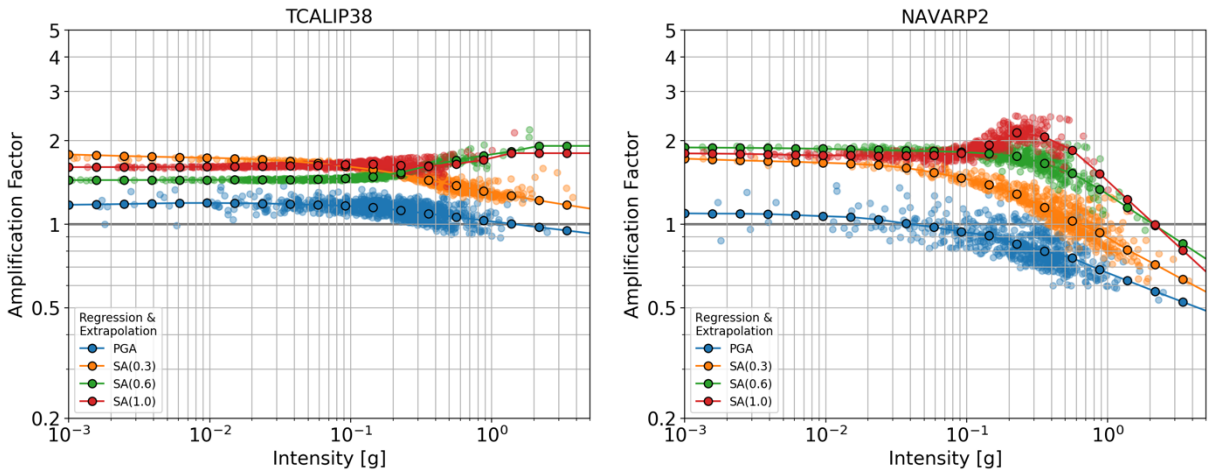

Figure 5: Example of simulated AFs using the same input motions at two different sites, a) one stiffer, with Vs30=418m/s (left) and b) one softer, with Vs30=273 m/s (right). The AFs were computed for four spectral periods (PGA, 0.3, 0.6 and 1.0 s) and black dots are the median AFs computed via LOWESS regression. The median AFs are extrapolated to large intensities following the procedure described in the text.

Since our goal is to apply the soil response model at any location within the city (i.e., at the locations of all the assets), we compute the AFs and σ_{lnAF} zone-wise, and not just at individual sites. The underlying assumption is that the soil response is similar within each zone. For each city, we use the zonation proposed in the original MZ study (Figure 1). Additionally, in Cali, we derive an alternative zonation, by grouping sites with similar site response using a hierarchical clustering approach. Sites are grouped based on the relative similarity of AFs for spectral acceleration at 0.3 s across all intensities (the period typically controlling the risk for residential buildings), resulting in 7 groups, which are then used to define the boundaries of the alternative microzones. We find that the alternative zonation broadly matches the zonation proposed in the MZ study. Although the alternative zonation is not used in the TREQ project, this method demonstrates how microzones can be defined exclusively from SRA results, which may be useful in future work if an existing zonation is not available.

To derive the AFs and uncertainty within each zone, we group the AFs of all sites located in the same zone. The median AF is computed using LOWESS regression (as before) but this time considering all sites within each zone, and the same for calculating σ_{lnAF}. The final values of σ_{lnAF} are therefore driven by the use of multiple input motions, and also the variability of the site response at different stations within each zone. For microzones containing only one station, the σ_{lnAF} may be underestimated, and in this case, we consider using a fixed minimum value of σ_{lnAF}=0.3 following Stewart et al. (2014), who compared the results of numerous simulation-based and data-based studies and recommend this value for periods between PGA - 3.0 s.

5.2 Hazard calculation

5.2.1 Combining bedrock hazard with soil response model

Hazard curves at the surface are computed using the numerical convolution approach (Bazzurro and Cornell, 2004, eq. 3) implemented in the OQ Engine, which combines the computed hazard curve on reference bedrock with the AF probability density function (i.e., the median AF and σ_{lnAF}). In the convolution approach, every ground motion intensity of the bedrock hazard curve contributes to the hazard at every ground motion intensity at the surface, according to the respective probabilities of exceedance. A benefit of the method is that it allows for incorporating uncertainty of the AF (i.e., σ_{lnAF}), although it should be noted that this approach treats all of the amplification uncertainty as aleatory.

For risk calculations, the soil amplification model is incorporated using a different approach. First a stochastic earthquake catalog is generated. For each event, a ground motion field is computed on reference bedrock, where the between and within-event components of ground motion variability are sampled separately if they are defined separately in the GMPE. For every site, the ground motion on reference bedrock is multiplied by a value sampled from the AF probability density function (i.e., the median AF and σ_{lnAF}) to obtain the ground motion at the surface.

5.2.2 Partially non ergodic approach for PSHA

The GMPEs are usually developed from ground motion data recorded or simulated for a certain region (host) and are widely used while conducting PSHA in other regions (target). The difference in the seismological characteristics between the host and the target region adds a certain amount of uncertainty. This is known as ergodic PSHA wherein the variability over time is substituted with variability over space. This uncertainty can be removed or at least reduced with the availability of region- or site-specific data. Consideration of alternate soil profiles with varying characteristics of VS, layer thickness, γ , G/Gmax and D curves and input motions can aid in quantifying the repeatable site effects.

In the present study, a partially non ergodic approach was adopted wherein a fraction of the site variability contributing to the total sigma of a GMPE is removed. In the present study, the variability associated with input motions alone is considered as inclusion of other variabilities was rendering the

LOWESS regression ineffective. The fraction estimated from incorporating the variability in input motion is removed from the standard deviation of the GMPE. For cities such as Santiago and Quito, wherein a single site was available for each microzone, the recommendation of Stewart et al., (2014) was followed and a standard value of 0.3 was removed from the standard deviation of the GMPE.

The practical application of the above discussed methodology can be performed on the OQ engine by modifying the GMPE logic tree. The fraction to be deducted from the standard deviation of the GMPE is estimated from Figure 5. The figure 5 shows the LOWESS fit for two sites in Cali for each IMT and GMPE. The difference between the fit and the individual response simulation is considered as σ_{lnAF}. The σ_{lnAF} averaged across all periods, intensity measure levels, and sites specific to each GMPE is calculated and the same factor is removed from the aleatory component of the GMPE in the logic tree, in order to avoid double counting the aleatory uncertainty due to site response. We do not remove the ergodic within-event variability, as commonly done in non-ergodic PSHA for a single site (e.g., Rodriguez-Marek et al., 2014) since we assume there still remains some site-to-site variability within the microzones. A typical example of the procedure used in this study is shown in Figure 6.

Further, the hazard computed with the reduced aleatory uncertainty is compared with the hazard curves at bedrock level and with full aleatory component in Figure 7. It can be seen that the hazard curve with reduced aleatory variability shows a lower POE across the entire range of intensity measure levels as compared to hazard curve with full aleatory component.

```
<!-- 3.0 Logic Tree for Interface Zone -->

        <logicTreeBranchingLevel branchingLevelID="_bl03">

            <logicTreeBranchSet branchSetID="_bs03" uncertaintyType="gmpeModel"
                    applyToTectonicRegionType="Subduction Interface">

                <logicTreeBranch branchID="b31">
                    <uncertaintyModel>
                        [ModifiableGMPE]
                        gmpe.AbrahamsonEtAl2015SInter = {}
                        add_delta_std_to_total_std.delta=-0.20
                    </uncertaintyModel>
                    <uncertaintyWeight>0.437</uncertaintyWeight>
                </logicTreeBranch>

                <logicTreeBranch branchID="b32">
                    <uncertaintyModel>
                        [ModifiableGMPE]
                        gmpe.ZhaoEtAl2006SInterNSHMP2008 = {}
                        add_delta_std_to_total_std.delta=-0.24
                    </uncertaintyModel>
                    <uncertaintyWeight>0.348</uncertaintyWeight>
                </logicTreeBranch>


                <logicTreeBranch branchID="b33">
                    <uncertaintyModel>
                        [ModifiableGMPE]
                        gmpe.MontalvaEtAl2017SInter = {}
                        add_delta_std_to_total_std.delta=-0.21
                    </uncertaintyModel>
                    <uncertaintyWeight>0.215</uncertaintyWeight>
                </logicTreeBranch>


            </logicTreeBranchSet>
        </logicTreeBranchingLevel>
```

Figure 6: Modified GMPE logic tree for the interface tectonic region type in Cali.

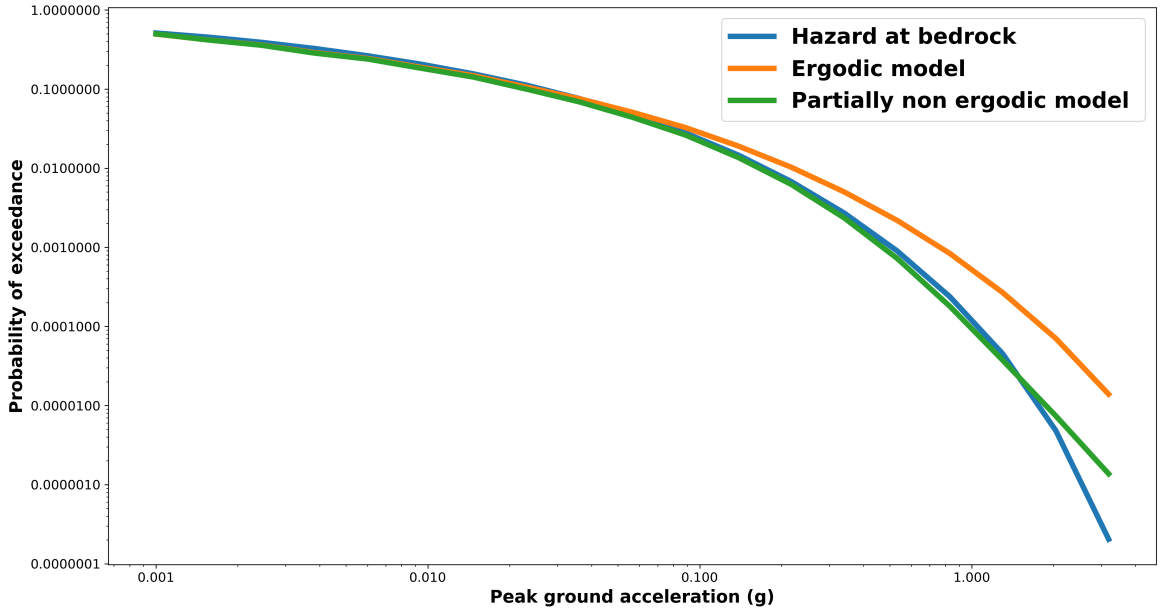

Figure 7. Comparison of the hazard results computed using different methods.

6 RESULTS

6.1 Soil response models

6.1.1 Cali

The soil response model for Cali is shown in Figure 8. The AFs were computed for all zones except zone 1 and zone 3, where data was not available. Since zone 1 is rock, we assume AF=1 for all intensities, and in zone 3, we assume the same AFs as zone 4A, due to similarities in the soil properties. In the western zones (2, 3, 4A, and 4B), which are characterized by rock and stiff soils, there is amplification at all periods and intensities, reaching 2.5 in zone 4a. In the eastern zones (4B, 4C, 4D, 5 and 6), which are characterized by soft soils, there is a prevalence of longer period (2.0 s) amplification, reaching a factor 2.5 in Zone 4C, and also a pronounced deamplification at short periods (i.e., PGA) with increasing bedrock shaking intensity. This deamplification is particularly strong in zone 6 (along with zones 4C and 5), which is the zone that has the largest impact on the risk. This deamplification is not present in the western zones, nor is it so prevalent in the other two cities.

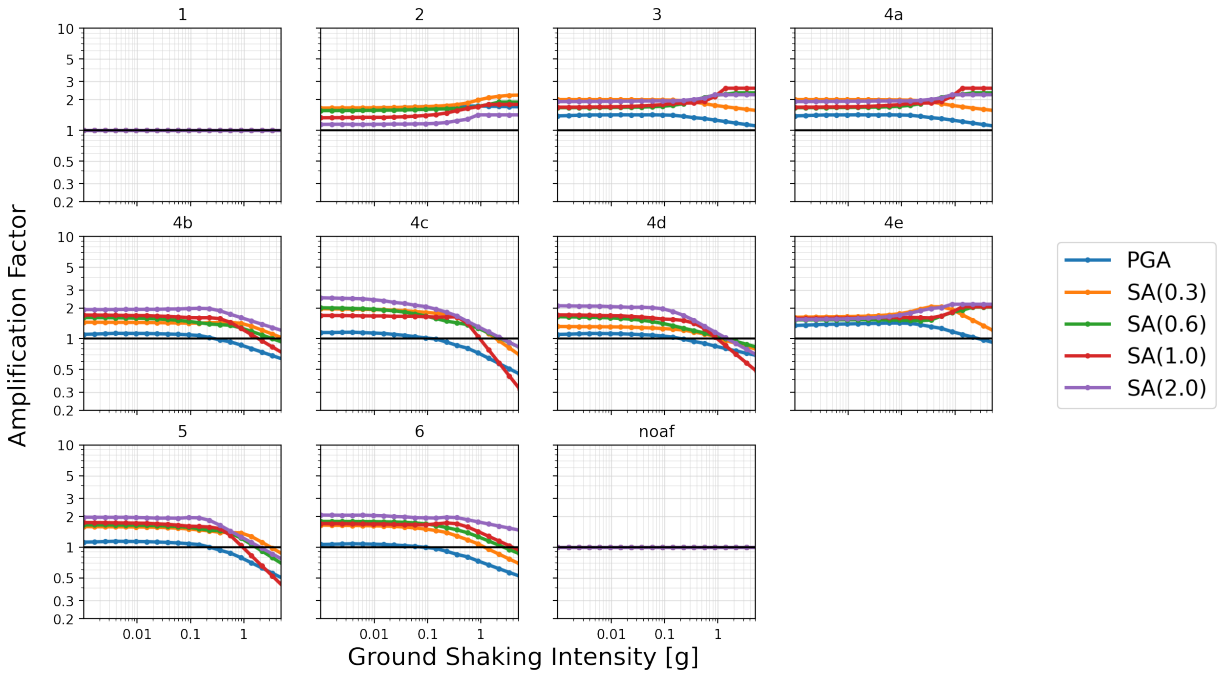

Figure 8: Soil response model for Cali showing the median AFs in each zone for different periods. The zone "noaf" is used for assets outside the microzones for which we assign AF=1 (no amplification) and an inferred Vs30 is used instead.

6.1.2 Quito

The soil response model for Quito is shown in Figure 9. All zones, with the exception of MSQ11, amplify at all periods and intensities, reaching up to a factor 5 in Zone MSQ3 at 2.0 s, the highest of the three cities. Unlike Cali and Quito, we cannot identify any general trends for the periods that amplify the most, because they are different at all sites. Focusing on zones MSQ2, MSQ10, and MSQ11, which are the zones that have the largest impact on the risk, we observe that they have notably different responses. Zone MSQ2 has a prominent amplification at 0.3 s, which remains above 2.5 up until 0.5 g. This is consistent with the impedance contrast at 20 m (Figure 3) which, given the Vs profile of the site, corresponds to a fundamental resonant period in line with the observed amplification at 0.3 s. Additionally, soil softening is not observed in this zone, implying higher AFs at large intensities compared to other zones. Zone MSQ11, on the other hand, exhibits soil softening with increasing bedrock shaking intensity and is the only zone where notable deamplification is observed at all frequencies (albeit at very large intensities > 1 g). This is consistent with this profile being the softest in Quito (Figure 3). Zone MSQ10 exhibits more moderate amplification, reaching a factor of 2.5 then decreasing (at all frequencies) down to a factor ~1 as shaking intensity increases.

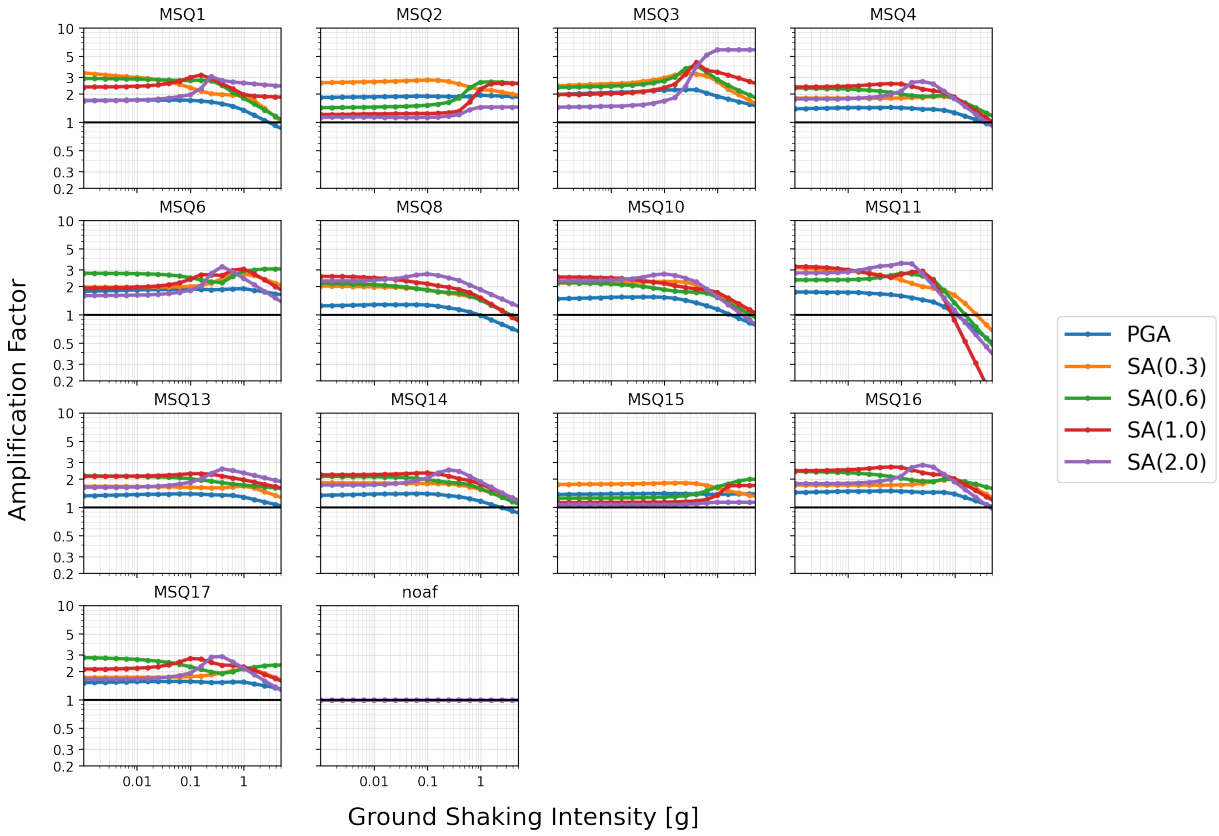

Figure 9: Soil response model for Quito showing the median AFs in each zone for different periods. The zone "noaf" is used for assets outside the microzones for which we assign AF=1 (no amplification) and an inferred Vs30 is used instead.

6.1.3 Santiago

The soil response model for Santiago is shown in Figure 10. All zones, with the exception of zones 1 and 7, amplify at all periods and intensities, reaching up to a factor 4 in Zone 8 at 1.0 s. Across all zones, there is a general trend of maximum amplification occurring at 0.3 s and 0.6 s. Focusing on zones 0, 1, 6, and 8, which are the zones that have the largest impact on the risk, we observe that they have notably different responses. Zone 1 (Licey clays) and zone 8 have the largest amplification at lower intensities (AFs between 1 and 3 depending on the period), while at high intensities, zone 8 has the largest amplification, as stated previously. Notably, this zone does not exhibit any soil softening (unlike zones 0, 1 and 6), and the soil column representing this zone is characterized by low Vs30 (253 m/s) and high plasticity. Zone 1 has the most deamplification of all the zones, with PGA demplifying above 0.1 g, while at 0.3 s and 0.6 s, the deamplification occurs above 0.4g. In zone 6, there is a broad amplification at all periods and intensities, especially at 0.6 s.

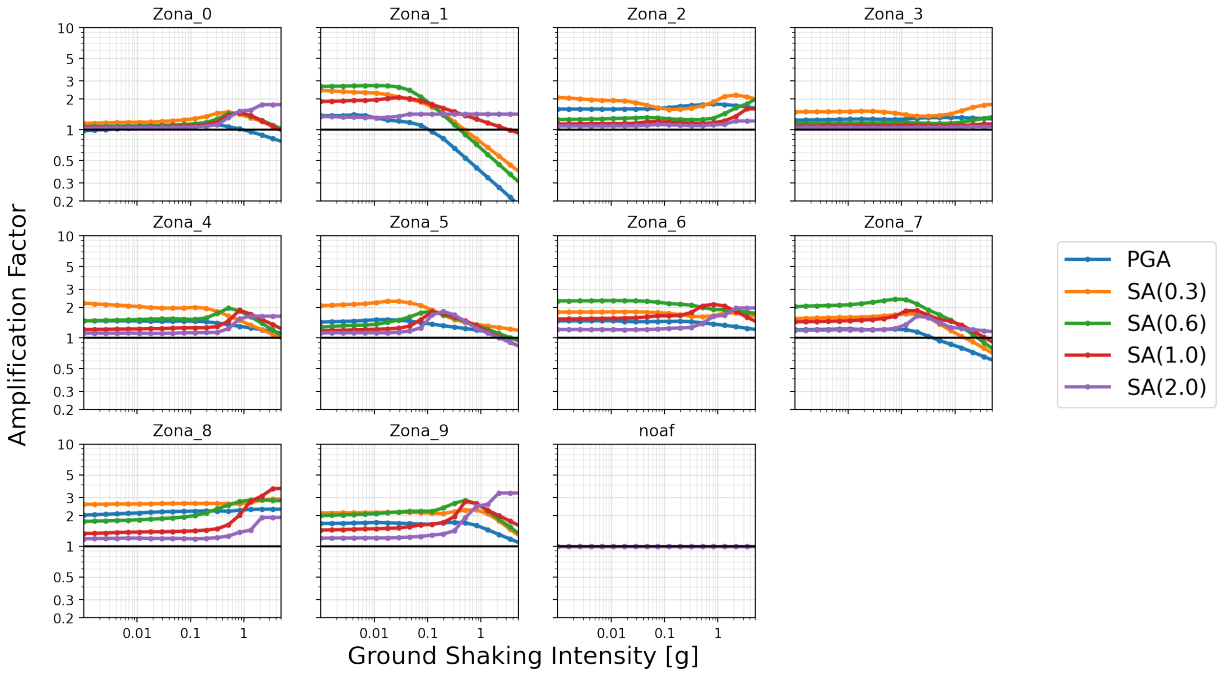

Figure 10: Soil response model for Santiago showing the median AFs in each zone for different periods. The zone "noaf" is used for assets outside the microzones for which we assign AF=1 (no amplification) and an inferred Vs30 is used instead.

6.2 Urban hazard

The most straightforward way to evaluate the impact of the AFs on the hazard is to compute hazard curves in each zone of each city. For this exercise, the location of the hazard curves is taken as the centroid of each zone. For each zone we compute (1) the hazard on reference bedrock (Vs30 = 800 m/s), (2) the hazard computed using the ergodic site term within GMPEs, which depend Vs30, and (3) the hazard computed using the AFs and convolution approach. The hazard models used are those described in Section 3.

6.2.1 Cali

The hazard curves in Cali are shown in Figure 11. The inferred Vs30 values are from the global model of Heath et al. (2020), in which the embedded map of Eraso (2015) covers Cali. The hazard curves computed using AFs are both higher and lower than the hazard curves computed using the ergodic site terms within the GMPEs. Cali is the only city where, for many zones, the hazard curves computed using AFs are lower than the hazard curves on rock at high intensities. The decrease in hazard is in the eastern zones (4B, 4C, 4D, 5 and 6), where there are AFs < 1 for large values of bedrock shaking intensity at short periods (Figure 8). Of the three cities, Cali has the lowest bedrock hazard (in terms of PGA, Figure 1), and after applying the AFs, the hazard curves on soil generally remain the lowest of the three cities (in terms of PGA).

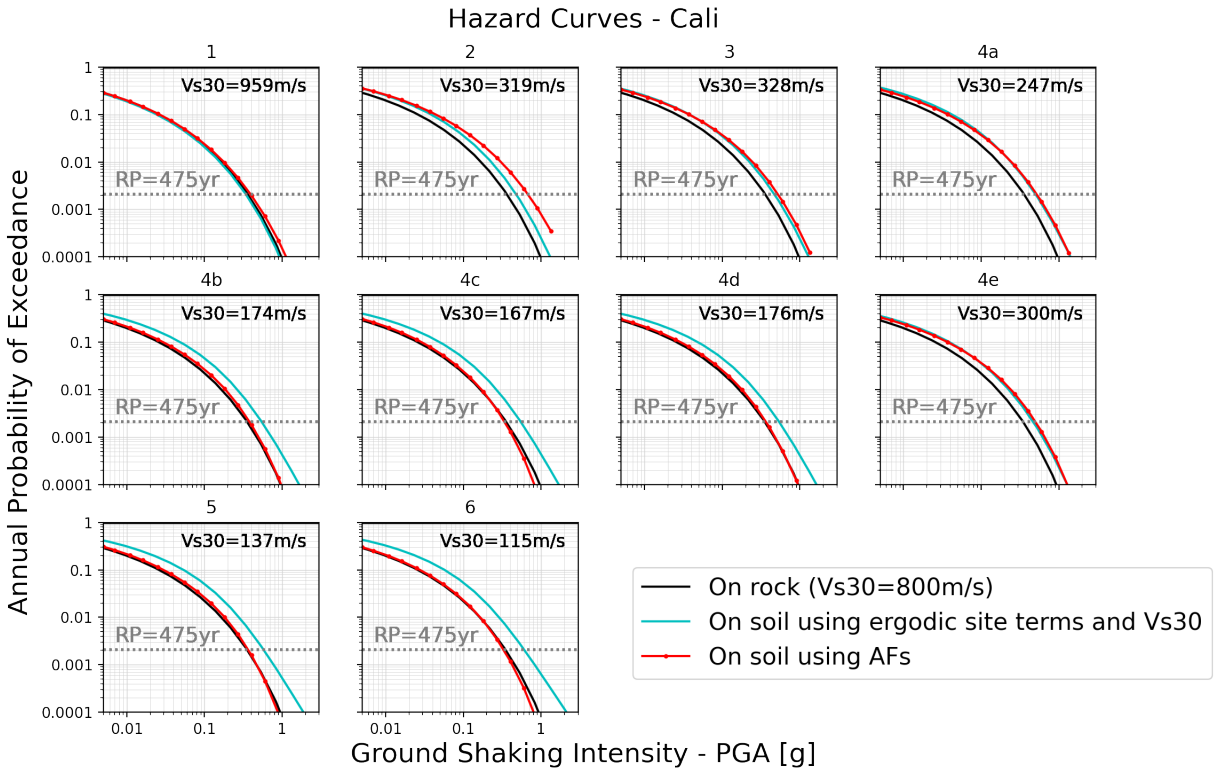

Figure 11: Hazard curves in Cali computed at the centroid of each zone. Curves are computed on rock (Vs30=800 m/s), on soil using ergodic site terms and Vs30 from Heath et al. (2020), and using the soil amplification model derived in this study (i.e., AFs and σ_{lnAF}).

6.2.2 Quito

The hazard curves in Quito are shown in Figure 12. The inferred Vs30 values are from the global model of Heath et al. (2020), in which the embedded map of Eraso (2015) covers Cali. With the exception of MSQ8, MSQ10 and MSQ11 at low POEs (~0.0001), the hazard curves computed using AFs are all higher than the curves computed using the ergodic site terms within the GMPEs. Of the three cities, Quito generally has the highest hazard (in terms of PGA) after applying the AFs.

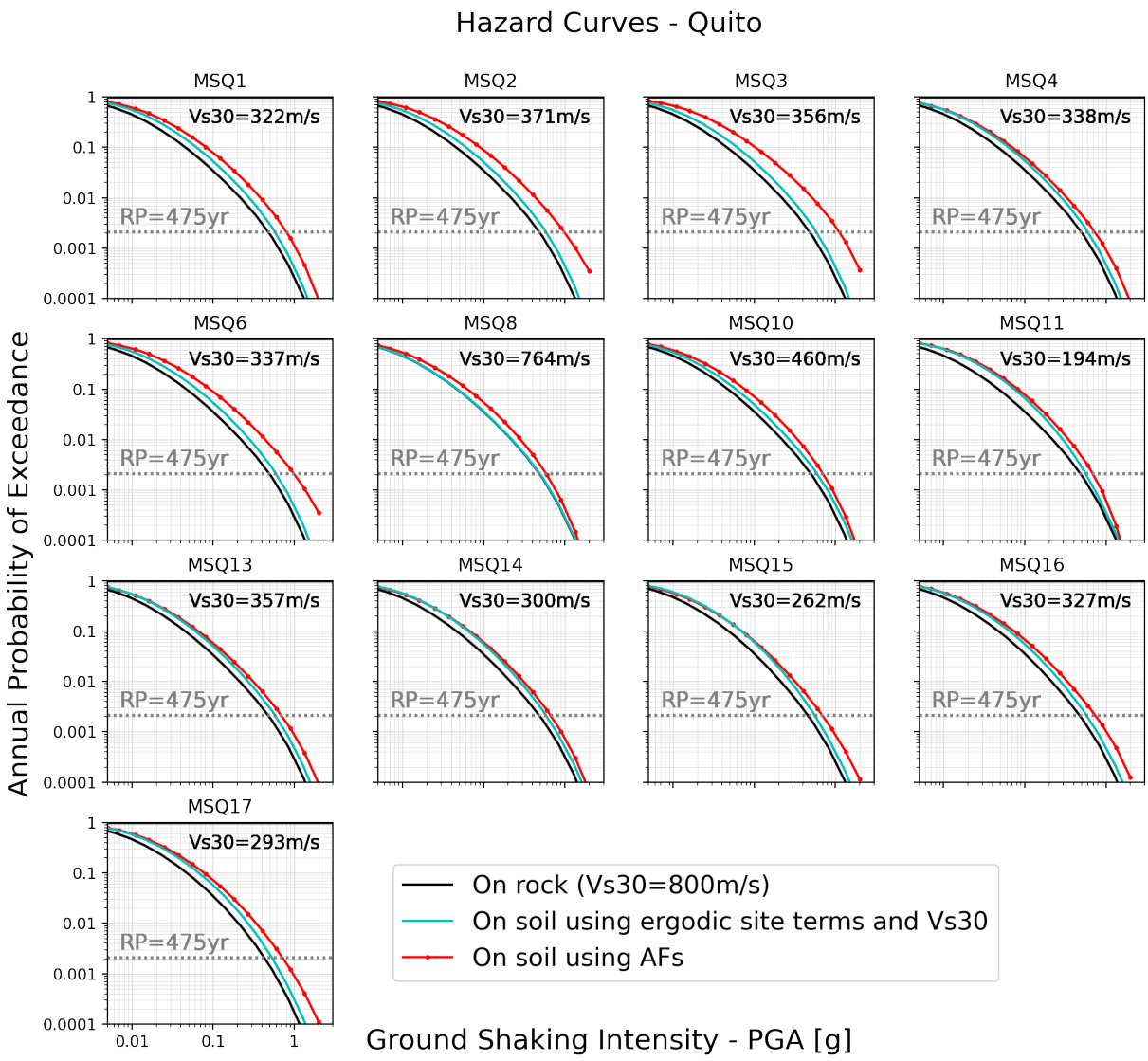

Figure 12: Hazard curves in Quito computed at the centroid of each zone. Curves are computed on rock (Vs30=800 m/s), on soil using ergodic site terms and Vs30 from Heath et al. (2020), and using the soil amplification model derived in this study (i.e., AFs and σ_{lnAF}).

6.2.3 Santiago

The hazard curves in Cali are shown in Figure 13. The inferred Vs30 values are from the global model of Heath et al. (2020), in which coverage in Santiago is the same as from Allen and Wald (2007). Depending on the zone, the hazard curves computed using AFs are either higher or lower than the curves computed using the ergodic site terms within the GMPEs. Of the three cities, Santiago has the highest bedrock hazard (in terms of PGA, Figure 1), and after applying the AFs, the hazard curves on soil are generally the highest of the three cities, although for some zones (i.e., zone 1) there is notable deamplification which reduces the hazard.

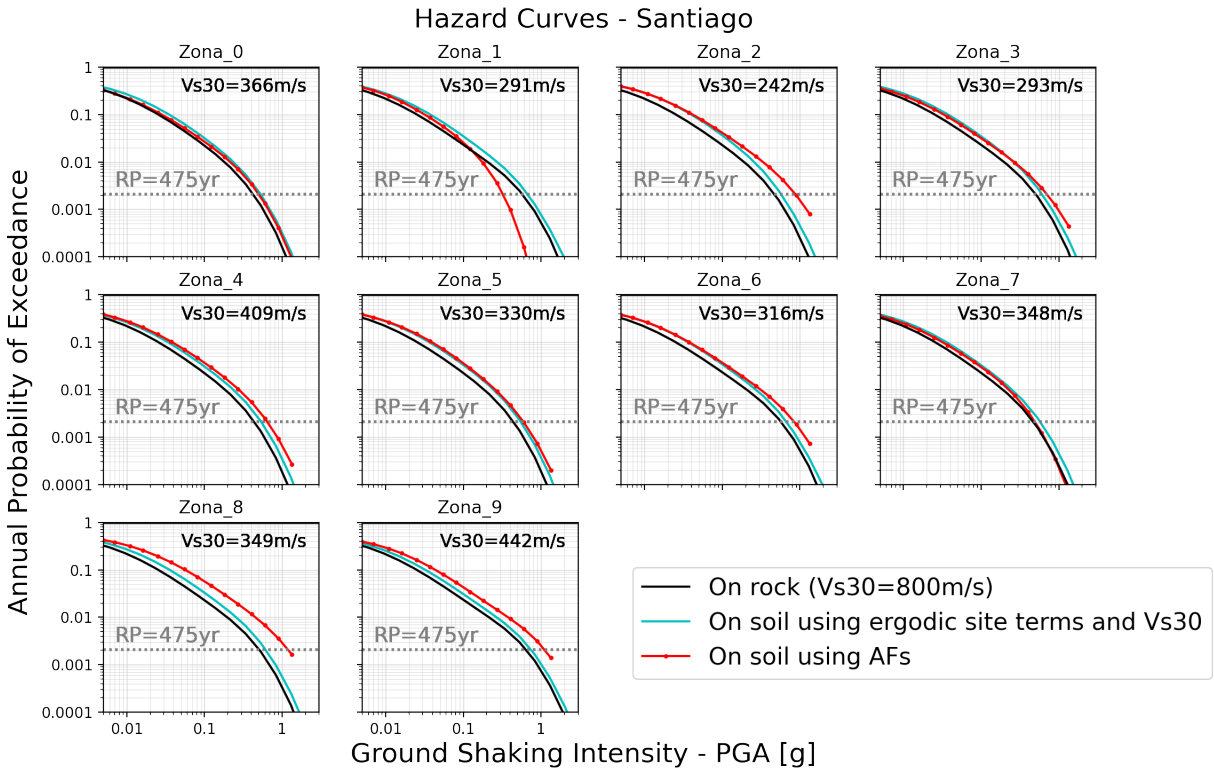

Figure 13: Hazard curves in Santiago computed at the centroid of each zone. Curves are computed on rock (Vs30=800 m/s), on soil using ergodic site terms and Vs30 from Heath et al. (2020), and using the soil amplification model derived in this study (i.e., AFs and σ_{lnAF}).

7 Discussion

7.1 Comparison of AFs with previous studies

In Cali, we can make a general comparison between the results of this study and the AFs computed by Ingeominas and Dagma (2005) (Informe 5.2, Annex 4), but not a direct comparison because their AFs were computed as a function of period, not ground shaking intensity on bedrock. Ingeominas and Dagma (2005) performed 1D equivalent linear SRA using ProSHAKE and DEEPSOIL using 10 time series with intensity ~0.2 g (according to Informe 5.2, Table 6.2). Similar to Ingeominas and Dagma (2005), we find amplification in the eastern zones at longer periods (2.0 s), amplification in the western zones at all periods, and deamplification in the eastern zones' short periods. A notable difference is that Zone 3 was modelled by means of 2D cross sections in Ingeominas and Dagma (2005), whereas here the values are taken from Zone 4a, as explained in Section 6.1.1.

In Quito, ERN et al. (2012) performed 1D equivalent linear SRA using SHAKE91 and 22 time series. The study computed response spectra at the surface (not AFs), and their results shown in Figure 4.12 are provided as a function of period, (although they considered a range of input motions intensities of 0.05, 0.1, 0.2 and 0.4 g). Similar to the ERN et al. (2012), we find that the response is quite variable within

the Quito basin, both spatially and in terms of the periods amplified. Our results indicate the highest AFs (> 3) in zones MSQ1, MSQ3, MSQ6 and MSQ11, while in ERN et al. (2012) find that the largest spectral peaks in zones MSQ8, MSQ10 and MSQ11. In the northern zone of MSQ2, which has a large impact on the risk, we find amplification at 0.3 s, but such a prominent peak is not observed in ERN et al. (2012) at this period. In the southern part of the basin, we observe that stations MSQ8, MSQ10, and MSQ1 reach maximum AF at 2.0 s, which in line with other studies that have indicated longer periods resonances in the south (e.g., Alfonso-Naya et al., 2012; Laurendeau et al., 2017).

In Santiago, only a general comparison with the results of Roullé et al. (2011) (Figures 20–35) is possible, because that study only computed response spectra at the surface (not AFs) as a function of period. Roullé et al. (2011) performed 1D equivalent linear SRA using CyberQuake using 8 time series. We do not find justification to group the 10 zones into 5 classes as done in their study (Figure 37), but we do observe some similarities with their results. Similar to Roullé et al. (2011), we find that zone 0 has the flattest response. In contrast to their results, we also observe moderate responses (i.e., AFs < ~2) in the adjacent zones (2, 3, 4), which are all in the west of the city, where the peak responses occur at ~0.3 s. In the east of the city (i.e., zones 1, 7, 8, 9), we find more pronounced amplifications at longer periods (0.3–0.6 s), which is in general agreement with the final spectra proposed by Roullé et al. (2011) (Figure 35). This is likely due to the presence of clays in the east of the city, which tend to amplify longer period motion, a finding which is also reiterated in Llorente et al. (2017).

7.2 Comparison of hazard curves computed using Vs30 vs AFs

Differences in the hazard curves computed using the AFs versus Vs30 (via the ergodic site terms in the GMPEs) can be explained by many reasons. Firstly, the simulated AFs can capture specific aspects of the local soil response, such as resonances and sediment behavior below 30 m, which are not captured by Vs30. Therefore, it is expected that the simulated AFs may be higher or lower than what is predicted by the ergodic site terms in the GMPEs, which depend on Vs30. Another contributing factor is the uncertainty of the Vs30 values themselves. Vs30 derived from topographic slope and other hybrid methods (Allen and Wald 2007; Health et al., 2020), is the standard and most practical way to estimate Vs30 for a large number of sites or assets, however these Vs30 values can differ from the measured values (Figure 1). A final explanation is that the ergodic site terms within GMPEs can differ up to a factor 10 in terms of predicted amplification (Stewart et al., 2015), and therefore the hazard results strongly depend on which GMPEs are used. For example, the GMPE of Idriss (2014), which is used in this study to compute the hazard in Colombia, is not recommended by the authors for soft sites (Vs30 < 450 m/s) because it does not model soil nonlinearity (i.e., a decrease in amplification with increasing bedrock shaking intensity). In Cali, the Vs30 values are well below this threshold, which explains why the hazard computed using Vs30 is much higher compared to when AFs are used (i.e., by not modelling nonlinearity there is an overestimation of the ground motion). These differences are likely exacerbated in Cali because the inferred Vs30 are even lower than the measured ones (Figure 1). This demonstrates a case where a GMPE – appropriate for national-scale hazard analysis on reference rock – may not be appropriate to use at the urban scale when soft sediments are present.

8 CONCLUSIONS

Using local geotechnical data, we developed soil response models and performed urban-scale hazard analysis for three cities in Latin America. This study not only highlights the impact of the local soil response on the final hazard curves for the three investigated cities, but also presents a methodological workflow for computing soil amplification factors that can easily be applied to other cities. The only two requirements of this approach are the availability of a PSHA hazard model and having sufficient geotechnical data to characterize the soil response across the urban centers. It should be emphasized that the methodological workflow presented here is generic, and that a more precise soil response model developed by local experts (for example using more detailed data and/or modelling techniques), could also be used to compute the hazard at the surface, for example in OQ.

Our results demonstrate the impact on the hazard of explicitly accounting for local soil response. We find that in some zones the hazard can be at least ~2x higher when AFs are used instead of the ergodic site-terms in the GMPEs, while in other zones the hazard can be even lower than on bedrock, notably at high levels of input shaking intensity. The former can be attributed to resonance effects in some zones, while the latter is due to soil nonlinearity, both of which are not always adequately captured by the ergodic site terms in GMPEs. This demonstrates the importance of using AFs derived from local data – specifically those that are intensity dependent – when the goal is to model hazard and risk with a high level of detail, rather than relying on GMPEs. For urban-scale studies where it is not possible to carry out SRA, we recommend selecting GMPEs with the most robust site terms, especially when dealing with soft sites.

The main challenges in this study were the quantity and quality of geotechnical data and accounting for uncertainties in the hazard analysis. For example, limitations in the geotechnical data required us to estimate SRA parameters (e.g., PI, OCR, bedrock depth) and make large assumptions about how to extend the profiles to depth, especially in Cali and Quito. The limited number of profiles per zone (with the exception of Cali) also made it difficult to estimate σ_{lnAF} within zones. Future work in these cities, or others, would benefit from incorporating more geotechnical and geophysical data to improve the quality of the analysis. Future work should also aim to quantify the epistemic uncertainty of the soil response (Rodrigues-Marek et al., 2020; Stewart et al., 2020), for example by accounting for uncertainty in the profiles, bedrock depth, and SRA modeling methods.

9 REFERENCES

Alfonso-Naya, V., F. Courboulex, L. F. Bonilla, M. Ruiz, M. Vallée, and H. Yépes (2012). A large earthquake in Quito (Ecuador): Ground motion simulations and site effects, 15th World Conf. on Earthquake Engineering, Lisbon, Portugal, Number 4475, 10 pp.

Allen, T.I., and Wald, D.J., 2007, Topographic slope as a proxy for global seismic site conditions (VS30) and amplification around the globe: U.S. Geological Survey Open-File Report 2007-1357, 69 p.

Ameri, G., Hollender, F., Perron, V., & Martin, C. (2017). Site specific partially nonergodic PSHA for a hard-rock critical site in southern France: adjustment of ground motion prediction equations and sensitivity analysis. Bulletin of Earthquake Engineering. https://doi.org/10.1007/s10518-017-0118-6.

Arcila, M. García, J., Montejo, J., Eraso, J., Valcarcel, J., Mora, M., Viganò, D., Pagani, M. y Díaz, F. (2020). Modelo nacional de amenaza sísmica para Colombia. Bogotá: Servicio Geológico Colombiano y Fundación Global Earthquake Model. https://doi.org/10.32685/9789585279469

Aristizábal C, Bard P-Y, Beauval C, Lorito S, Selva J et al (2016). Guidelines and case studies of site monitoring to reduce the uncertainties affecting site-specific earthquake hazard assessment. Deliverable D3.4—STREST—harmonized approach to stress tests for critical infrastructures against natural hazards. http://www.strest-eu.org/opencms/opencms/results/

Bazzurro, P. and Cornell, C. A. (2004). Ground-Motion Ampli cation in Nonlinear Soil Sites with Uncertain Properties. Bulletin of the Seismological Society of America, 94:2110–2123, 2004.

Beauval C., J. Marinière, H. Yepes, L. Audin, J.-M. Nocquet, A. Alvarado, S. Baize, J. Aguilar, J.-C. Singaucho, H. Jomard (2018). A New Seismic Hazard Model for Ecuador. Bulletin of the Seismological Society of America; 108 (3A): 1443–1464. doi: https://doi.org/10.1785/0120170259

Castro Villamarín, N. (2011). Evaluación de la respuesta sísmica no-lineal de un depósito de suelo pre-consolidado de la ciudad de Cali., Ph.D. Thesis, Universidad Nacional de Colombia, Bogotá

Darendeli, M. B. (2001). Development of a new family of normalized modulus reduction and material damping curves, Ph.D. Thesis, The University of Texas, Austin.

EPRI (2013) Seismic evaluation guidance. Screening, prioritization and implementation details (SPID) for the resolution of Fukushima near-term task force recommendation 2.1. Seismic. EPRI report no. 1025281, December. Palo Alto, CA: Electrical Power Research Institute.

Eraso J. Cálculo del Promedio de Velocidad de Onda de Corte a 30 Metros de Profundidad (Vs30) En Colombia Como una Aproximación a la Estimación de los Efectos Sísmicos de Sitio a Escala Nacional [Report] / Servicio Geológico Colombiano. - Bogotá: [s.n.], 2015. - p. 28.

EPN (1994). The Quito, Ecuador, Earthquake Risk Management Project: An Overview. GeoHazards International Publication, San Francisco, USA.

ERN (2012). Microzonificación sísmica del distrito metropolitano de Quito: Estudio de la amenaza sísmica a nivel local.

Guéguen, P. (1997). Microzonificación de Quito (Ecuador). Institut Francais de Recherche Scientifique pour le Développement en Coopération (ORSTOM) and Instituto Geofísico, Escuela Politécnica Nacional.

Heath, D., Wald, D. J., Worden, C. B., Thompson, E. M., and Scmocyk, G. (2020). A Global Hybrid VS30 Map with a Topographic-Slope-Based Default and Regional Map Insets", Earthquake Spectra, vol. 36, 3: pp. 1570-1584.

Idriss, I. (2014). An NGA-West2 empirical model for estimating the horizontal spectral values generated by shallow crustal earthquakes. Earthquake Spectra, 30 (3), 1155-1177. http://dx.doi.org/10.1193/072813EQS219M.

Ingeominas and Dagma (2005). Estudio de microzonificación sísmica de Santiago de Cali. Bogotá. Ministerio de Minas y Energía.

Kaklamanos, J., B. A. Bradley, A. N. Moolacattu, and B. M. Picard (2020). Physical hypotheses for adjusting coarse profiles and improving 1D site-response estimation assessed at 10 KiK-net sites, Bulletin of the Seismological Society of America, Vol. 110, No. 3, pp. 1338–1358. https://doi.org/10.1785/0120190263.

Kamai, R. , Abrahamson, N. A. , and Silva, W. J. , 2014. Nonlinear horizontal site amplification for constraining the NGA-West2 GMPEs, Earthquake Spectra 30, 1223–1240.

Kausel E, Assimaki D (2002) Seismic simulation of inelastic soils via frequency-dependent moduli and damping. ASCE j Eng Mech 128:34–47.

Kottke, A. and Rathje, E. (2009). Technical Manual for Strata. PEER Report 2008/10. University of California, Berkeley, California.

Kottke, A, & Stickler Bot. (2019). arkottke/pysra v0.4.5 (v0.4.5). Zenodo. https://doi.org/10.5281/zenodo.3522104.

Kottke, A. and Rathje, E. (2013). Comparison of time series and random-vibration theory site-response methods. Bull Seismol Soc Am 103(3):2111–2127.

Laurendeau, A., Courboulex, F., Bonilla, L. F., Alvarado, A.,Alfonso, Naya V., Mercerat, D., et al. (2017). Low frequencyseismic amplification in the quito basin (ecuador) revealed by accelerometric recordings of the RENAC network.Bulletin of theSeismological Society of America, 107(6), 2917–2926.

Leon, A. (2018). Generacion de mapas Vs30 y microzonas sismicas en el distrito metropolitano de Quito, Ecuador, proyecto de grado, Universidad Simón Bolívar.

Llorente Isidro, M., Belvaux M., Bernardez E., Bertil D., Fernandez-Merodo J., Lain-Huerta L., Lopera-Caballero E., Muños-Tapia S. and Roullé A. (2017). Geología para el estudio de microzonación

sísmica en Santiago de los Caballeros, República Dominicana. Boletín Geológico y Minero, 128 (3): 715-736, ISSN: 0366-0176, DOI: 10.21701/bolgeomin.128.3.010.

Mayne, P.W. 2001. Stress-strain-strength-flow parameters from seismic cone tests. In Proceedings of the International Conference on In-Situ Measurement of Soil Properties & Case Histories, Bali, Indonesia. pp. 27–48.

Menq, F. Y. (2003). Dynamic properties of sandy and gravelly soils, Ph.D. Thesis, Department of Civil Engineering, University of Texas, Austin, Texas.

Moon, S.W. and Ku, T. (2016), "Development of global correlation models between in situ stress-normalized shear wave velocity and soil unit weight for plastic soils", Canadian Geotech. J., 53(10), 1600-1611. https://doi.org/10.1139/cgj- 2016-0015.

Pagani M, Monelli D, Weatherill G, Danciu L, Crowley H, Silva V, Henshaw P and Butler L (2014). OpenQuake Engine: An open hazard (and risk) software for the Global Earthquake Model. Seismological Research Letters 85: 692–702.

Pagani M, Garcia-Pelaez J, Gee R, Johnson K, Silva V, Simionato M, Styron R, Vigano D, DanciuL, Monelli D, Poggi V and Weatherill G (2020). The 2018 version of the Global EarthquakeModel: Hazard component.Earthquake Spectra. DOI: 10.1177/8755293020931866.

Rathje, E. M., Kottke, A. R., and Ozbey, M. C. (2005). "Using inverse random vibration theory to develop input Fourier amplitude spectra for use in site response." Proc., 16th Int. Conf. on Soil Mechanics and Geotechnical Engineering: TC4 Earthquake Geotechnical Engineering Satellite Conf., Osaka, Japan, 160–166.

Rathje, E. M., and M. C. Ozbey (2006). Site-specific validation of random vibration theory-based seismic site response analysis, J. Geotech. Geoenviron. Eng. 132, no. 7, 911–922.

Rodriguez-Marek, A. , Kruiver, P. P. , Meijers, P. , Bommer, J. J. , van Elk, J. , and Doornhof, D. , 2017. A regional site-response model for the Groningen gas field, Bulletin of the Seismological Society of America 107, 2067–2077.

Rodriguez-Marek A, Rathje EM, Bommer JJ, Scherbaum F and Stafford PJ (2014) Application of single-station sigma and site response characterization in a probabilistic seismic hazard analysis for a new nuclear site. Bulletin of the Seismological Society of America 104(4): 1601–1619.

Rodriguez-Marek, A., J. Bommer, R. R. Youngs, M. Crespo, P. Stafford, and M. Bahrampouri (2020). Capturing epistemic uncertainty in site response. Earthquake Spectra.

Roullé A., Vanoudheusden E., Belvaux M., Auclair S. (2011) – Microzonificación sísmica de Santiago – Republica Dominicana. Amenaza sísmica local. Informe final. BRGM/RC-59685-FR, 101 p., 43 fig., 11 tablas, 2 anexos.

Stewart, J.P., Afshari, K., and Hashash, Y. M. A., 2014. Guidelines for performing hazard-consistent one-dimensional ground response analysis for ground motion prediction, PEER Report No. 2014/16, Pacific Earthquake Engineering Research Center, UC Berkeley, CA.

Stewart, J. P., J. Douglas, M. Javanbarg, N. A. Abrahamson, Y. Bozorgnia, D. M. Boore, K. W. Campbell, E. Delavaud, M. Erdik, and P. J. Stafford (2015). Selection of ground motion prediction equations for the global earthquake model, Earthq. Spectra doi: 10.1193/013013EQS017M.

Stewart, J.P.; Afshari, K. (2020). Epistemic Uncertainty in Site Response as Derived from One-Dimensional Ground Response Analyses. J.Geotech. Geoenviron. Eng. 147, 04020146.

SM Working Group (2015). Guidelines for seismic microzonation, conference of regions and autonomous Provinces of Italy—Civil Protection Department, Rome, https://www.centromicrozonazionesismica.it/it/download/category/9-guidelines-for-seismic-microzonation. Last Accessed October 2021 (Original Italian Edition: Gruppo di lavoro MS, Indirizzi e criteri per la microzonazione sismica, Conferenza delle Regioni e delle Province autonome—Dipartimento della protezione civile, Roma, 2008, 3 vol. e Dvd).

Tromans, I.J., Aldama-Bustos, G., Douglas, J., Lessi-Cheimariou, A., Hunt, S., Daví, M., and Robertson, C. (2019). Probabilistic seismic hazard assessment for a new-build nuclear power plant site in the UK. Bulletin of Earthquake Engineering, 17(1), 1-36. https:// doi.org/10.1007/ s10518-018-0441-6.

United Nations, Department of Economic and Social Affairs, Population Division (2019). World Urbanization Prospects: The 2018 Revision (ST/ESA/SER.A/420). New York: United Nations.

Villagómez, D. (2003). Evolución geológica Plio-Cuaternaria del Valle Interandino central en Ecuador (zona de Quito-Guayllabamba-San Antonio), Eng. Thesis, Escuela Politécnica Nacional-Facultad de Geología, Quito Ecuador, 133.